

# Vortex dynamic, pinning and irreversibility field investigation in $EuRbFe_4As_4$ superconductor.

V.A. Vlasenko<sup>1</sup>, K.S. Pervakov<sup>1</sup>, S.U. Gavrilkin<sup>1</sup>

<sup>1</sup>P.N. Lebedev Physical Institute of RAS, 119991, Moscow, Russian Federation

**Abstract.** We performed systematic AC susceptibility and magnetic moment measurements to investigate the vortex dynamics and pinning in a  $EuRbFe_4As_4$  single crystal as a function of temperature, frequency and DC magnetic field. The vortex solid to vortex liquid line was determined and well fitted by  $H(T_p) = H_0(1 - t_p)^b$  with  $b=1.74-1.91$  for  $H \parallel c$  indicating rather high pinning strength of vortex system. The field dependence of the activation energy  $U_0$  is gained within the approach of thermally activated flux creep theory. A power law dependence of  $U \sim H^a$  with  $a = 0.52$  is observed below 1T. The activation energy reaches 6700K at low fields, suggesting strong pinning in the material. Magnetic moment measurements also confirms the strong pinning in  $EuRbFe_4As_4$ . We show  $Eu^{2+}$  magnetic ordering suppressed in magnetic fields about 3T.

**PACS numbers:** 74.70.Xa, 74.25.Bt, 74.25.-q, 74.25.Dw, 74.25.Nf, 74.25.Qt, 74.25.Wx

## 1. Introduction

Recently novel family of the Fe-based superconductors was discovered. It is so-called 1144-type ( $AeAFe_4As_4$ , whereas Ae = Ca, Sr, Ba, Eu and A = K, Rb, Cs) compounds [1]. The 1144 family exhibit intriguing and distinctive properties, which are currently in the research focus in the field of high temperature superconductors. The self doped  $AeAFe_4As_4$  [2] compounds possesses a tetragonal structure (P4/mmm), where Ae and A layers forming two inequivalent  $ThCr_2Si_2$  structures [1]. In contrast to 122 superconductors, Fe-As bonds have a different length between the As atoms and the Fe plane. The 1144 family displays superconductivity with superconducting transition temperature  $T_c$ , from 24K to 36 K [1, 3–5] and estimated upper critical fields from 92T [6] up to 250T [2]. Various transport, thermal, and thermodynamics experiments on 1144 system evident for the absence of any structural transition [7]. However, in the case of  $Eu(Rb/Cs)Fe_4As_4$ , the bulk superconductivity with  $T_c$  about 36 K, coexist with the  $Eu^{2+}$  spin localization, which leads to magnetic ordering at  $T_m$  about 15K. In contrast to the related 122-type compound ( $EuFe_2As_2$ ), whereas the antiferromagnetic order competes with the superconductivity, the magnetic order in 1144 system has a little influence on superconductivity [8]. The possible reason for such feature may be the significant spatial separation in the crystal structure of superconducting and magnetic planes. This exotic but distinctive behaviour in 1144 encourage the community to bridge up the knowledge gap in such unusual superconducting systems.

To date, there is a little data concerning the vortex dynamics, pinning and irreversibility line behaviour in  $EuRbFe_4As_4$  (Eu-1144) superconducting compounds. Therefore, the motivation was to investigate the physical properties and vortex matter features of the  $EuRbFe_4As_4$  single crystal.

## 2. Experimental details

$EuRbFe_4As_4$  single crystals were grown using the self-flux method as it has been done previously for Ni-doped Ba-122 [9, 10]. The initial high purity components of Eu (99.95%), Rb (99.99%) and FeAs (99.98% Fe + 99.9999% As) were mixed in 1:1:12 molar ratio, placed in an alumina crucible and sealed in a niobium tube under 0.2 atm of residual argon pressure. The sealed container was loaded into a tube furnace with an argon atmosphere. Next, the furnace was heated up to  $1250^{\circ}C$ , held at this temperature for 24h to homogenize melting and then cooled down to  $900^{\circ}C$  at a rate of  $2^{\circ}C/h$ . At this temperature, the ampoule with crystals was held for 24h for growth defects elimination and then cooled down to room temperature inside the furnace. Finally, crystals of size more than  $5 \times 5 \text{ mm}^2$  in the ab-plane were collected from the crucible. In the inset of Fig.1 the synthesized 1144 single crystals are presented. It is clearly seen that the cleaved surface of the  $EuRbFe_4As_4$  single crystal is smooth and clean. Obtained crystals were cleaved to 0.1-0.2  $\text{mm}^2$  thickness and cut into a rectangular shape for the following measurements. In this work, we use square shape single crystal with dimensions ( $a \times b \times c$ )

1.12mm, 0.65mm, and 0.12mm, respectively. Single crystal quality was investigated by complementary methods. The chemical composition of 1144 crystals was studied by a JEOL 7001F scanning electron microscope (SEM) with INCA X-act EDS attachment. The data from several points were averaged to improve the measurement accuracy. The elemental analysis mapping showed a uniform distribution of elements with the approximate chemical compositions of Eu-1144 phase ( $EuRbFe_4As_4$ ) on the surface (not presented here). In Fig.1 shown the temperature dependence of the  $EuRbFe_4As_4$  single crystal DC magnetization. Superconducting transition shape of crystal is similar to presented in ref. [12], manifesting high sample quality. We define the critical temperature ( $T_c = 34.8K$ ) of the superconducting transition using the onset criteria. The  $T_c$  of Eu-1144 sample is a bit lower than reported in ref. [11], but similar to presented in ref. [3]. The decrease in  $T_c$  can be explained by the existence of Rb deficiency (self-doping) which leads to extra hole-like charge carries and induces non-optimal doping regime in the sample [13]. A magnetic feature at about  $T_m = 15K$  was observed and it can be possibly related to the magnetic ordering [4]. The origin of observed ordering is mostly due to the spin localization on  $Eu^{2+}$  atoms. Therefore,  $EuRbFe_4As_4$  is found to be a ferromagnetic superconductor with Eu domains within the  $ab$  plane ordering according to the ref. [13, 14]. However, such features can be observed only in the magnetic measurements data indicates spatial separation and coexistence of magnetic and superconducting regions [8]. We found that the  $Eu^{2+}$  magnetic ordering is suppressed in fields about 3T, as it was shown in Fig.2.

It should be mentioned that  $EuRbFe_4As_4$  single crystals become tarnish while were exposed to air. The electron microscope investigation of Eu-1144 single crystal (see Fig.1) evident to the rubidium deficient caused by the oxidation within 1-hour air deposition. The repeated AC susceptibility measurements show a significant decrease in the diamagnetic signal after air deposition. We suggest the rubidium hydroxide formation on the surface of crystals causes rubidium loss in the bulk.

AC-susceptibility ( $\chi', \chi''$ ) and magnetic moment  $M(H)$  measurements were performed by using the Quantum Design PPMS-9 system. The magnetic susceptibility measurements were done in field-cooled (FC) conditions with  $H_{ac} = 1Oe$  and external magnetic field (H) up to 9T. The frequency ( $\nu_m$ ) range of  $H_{ac}$  varied from 33 to 9777Hz.

### 3. Results and discussions

To investigate vortex pinning matter in Eu-1144, it is necessary to discuss the interaction between magnetic and superconducting layers. It seems possible to use magnetic susceptibility and magnetic moment data in the models for conventional superconductors in case if the magnetic layers and superconducting condensate exhibit quasi-isolated behaviour. The facts confirming the weak interaction between the superconducting region and europium magnetic layers in  $EuRbFe_4As_4$  are as follows [14]: i) It was shown that magnetic vortices density didn't change much during  $Eu^{2+}$  ordering. ii) Magnetic ordering can be observed only within  $ab$  plane. iii) Europium replacement for non-

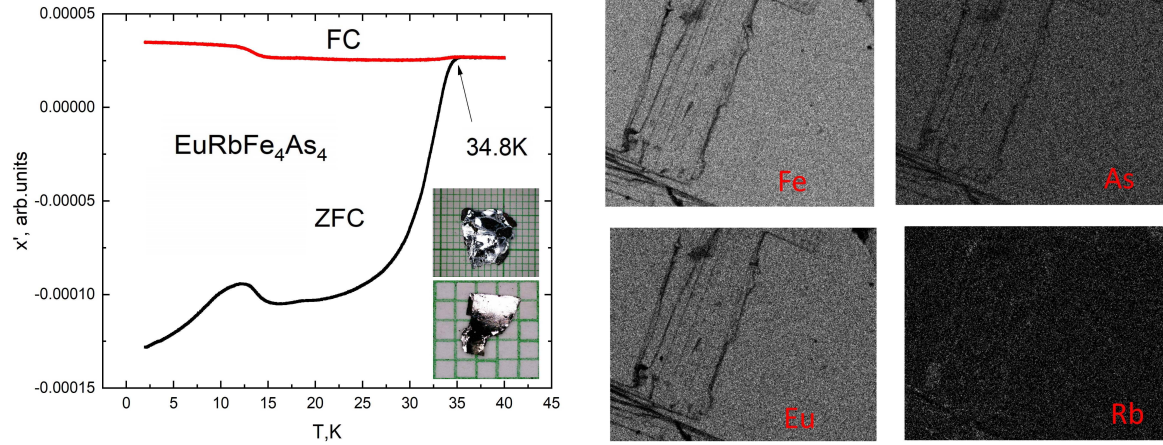


**Figure 1.** (Left) The temperature dependence of the DC ZFC (zero-field cooled) and FC magnetization in an external field of 10 Oe applied along the  $c$  axis. (Right) The elements distribution on the surface of Eu-1144 single crystal obtained by an electron microscope using INCA attachment after 1-hour deposition on the air. (Inset) Picture of the  $\text{EuRbFe}_4\text{As}_4$  single crystals are over a millimetre grid.

magnetic caesium leads only to magnetic ordering suppression, but superconducting transition curves remains almost unchanged. iv) The europium atoms are spatially isolated from superconducting layers. Thus, it is possible to provide magnetic studies with minimal distortion induced by europium in Eu-1144 superconductor.

We investigate vortex pinning matter in Eu-1144 by isothermal magnetization measurements  $M(H)$  presented in Fig.3. All  $M(H,T)$  data were collected with magnetic field parallel to the  $c$  axis. The linear-like  $M(H)$  curve at  $T > T_{sc}$ , indicates the presence of magnetic impurities. In the inset of Fig.3 is shown a low field data of magnetization loop near the  $T_c$ . Magnetic shielding of superconducting layers clearly overlapped Eu magnetic background lower than 34K. The  $\text{Eu}^{2+}$  magnetic ordering at about 15K leads to more  $S$ -shaped form of hysteresis loop, which indicates ferromagnetism appearance [13]. Nevertheless, the influence of intrinsic magnetism on  $M(H)$  irreversibility curve width is insignificant compared to SC phase shielding even at  $T < 15K$ . Since the  $M(H)$  width didn't vastly change before and after 15K, we may conclude that SC shielding gives the main contribution to the  $M(H)$  hysteresis.

In general magnetic superconductors have complex interplay between magnetism and superconductivity results in complexity of direct quantitative estimation of  $J_c$ . However, the qualitative conformity remains [16]. Therefore, we calculated  $J_c(H)$  at different temperatures using Beans critical state model [15]. According to the theoretical predictions  $J_c \sim D\Delta M(1)$ , where  $\Delta M$  is the magnetization measured with decreasing and increasing fields and  $D$  is the sample's geometrical factor. To avoid speculations about real value of critical current, we plot the  $J_c(H)$  in arbitrary units as it shown in inset of Fig.4.

In Fig. 4 one can see  $J_c$  data analysed according to the method mentioned in

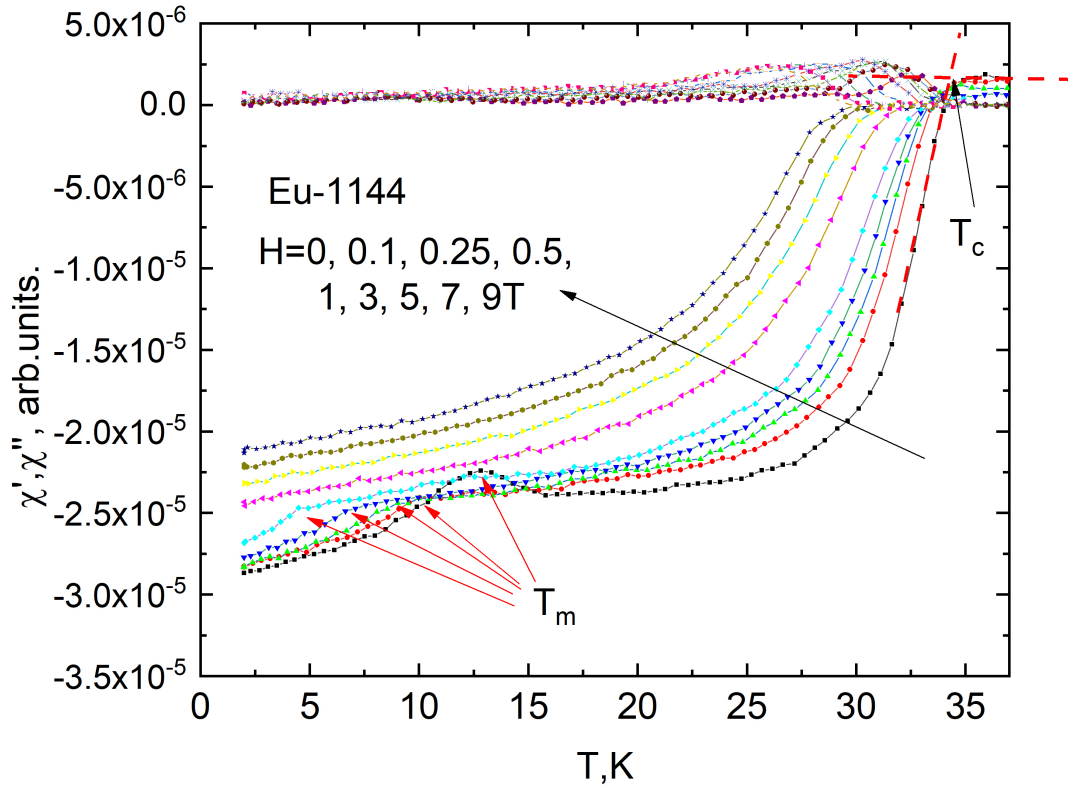


**Figure 2.** Temperature dependence of the in-phase and the out-of-phase AC susceptibility for  $H \parallel ab$  at various applied magnetic fields with the  $H_{ac} = 1$  Oe and a frequency  $\nu = 1333$  Hz.

ref. [17, 18]. Haberkorn et al. [17, 18] identified several pinning regimes from the  $J_c(H)$  diagram in the log-log scale. At low fields, typically less than 500 Oe,  $J_c$  is independent of external field – regime I. With the following  $H$  increasing one can observe a power law behaviour  $J_c \propto H^{-a}$  (regime II). Regime III manifests when  $J_c(H) \sim \text{const.}$  At last, regime IV can be observed when  $J_c$  rapidly tends to zero with  $H$  incrementing. The low-field part associated with the single vortex state regime. The  $J_c \propto H^{-a}$  dependencies due to the strong pinning centres and following III regime coheres with fishtail effect. A rapid decrease of  $J_c$  related to changes in the vortex dynamics. In order to check the presence of strong pinning in Eu-1144,  $J_c$  versus  $H$  on a log-log scale at different temperatures was plotted and the exponent  $a$  was estimated as it shown in the inset of Fig.4. Obviously, we observe a different  $J_c(T)$  behaviour in the low- and high-field data. The regime I evidently appears at fields less than 100 – 350 Oe. In higher magnetic fields up to 1.5 T the critical current follows a power law behaviour  $J_c \propto H^a$  with  $0.55 < a < 0.65$ . The  $a$  exponent values obtained in this work are in a good agreement with the theoretical prediction of  $H^{-5/8}$ , which indicates strong vortex pinning [19]. Further increase of the magnetic field leads to IV regime appearance, whereas the  $J_c$  decrease not so fast with

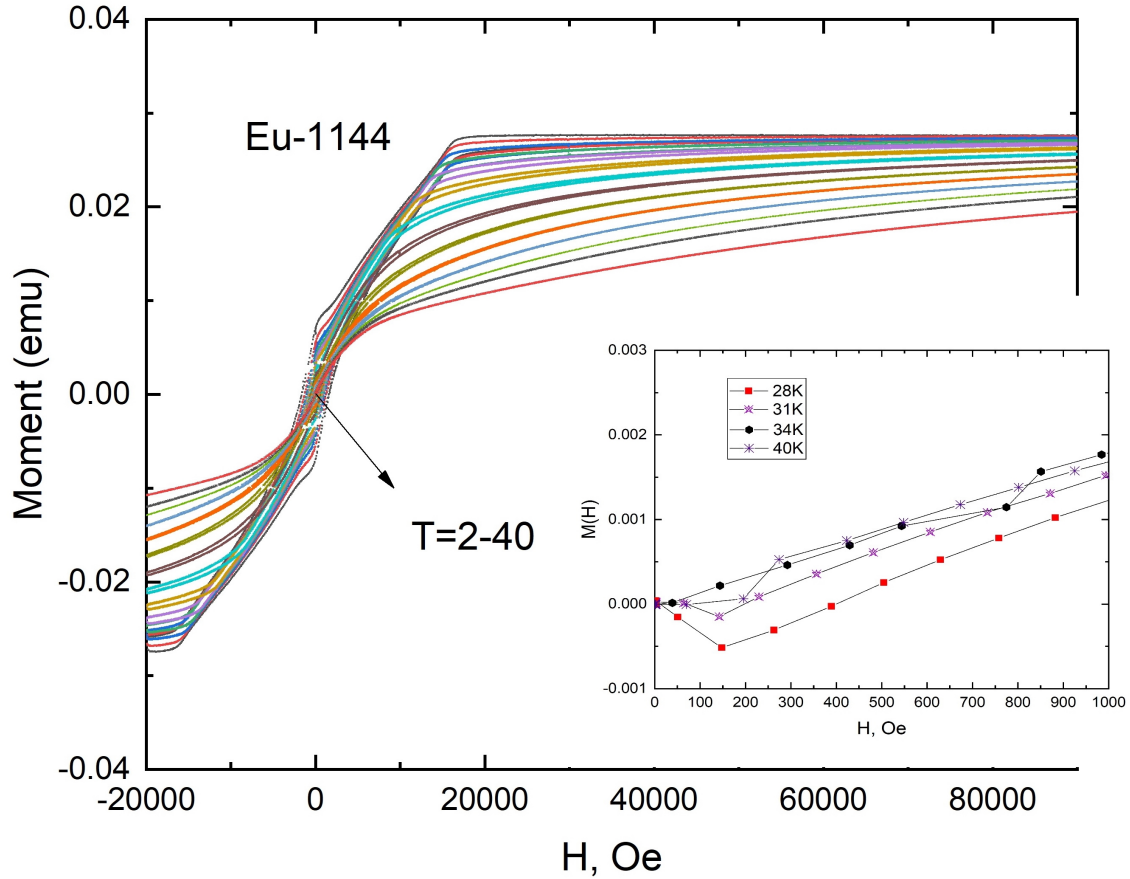


**Figure 3.** Isothermal magnetization hysteresis loops as a function of magnetic field with  $H \parallel c$  up to 9T are shown for Eu-1144.(Inset) Low field data of magnetization loop for temperatures below and above than the  $T_c$ .

an increase in the magnetic field indicating a rather high value of the irreversibility field ( $H_{irr}$ ).

Vortex dynamics and pinning can be studied by  $AC$  susceptibility measurements [20–23]. The  $AC$  susceptibility measurements data ( $\chi'$  and  $\chi''$ ) can be interpreted within the theory of thermally activated flux motion and collective vortex pinning in the assumption, as it was mentioned earlier, that the magnetism has weak influence on superconducting properties. It is generally accepted that  $\chi'$  is related to the ability of the magnetic flux shielding, and  $\chi''$  - with the dissipation mechanism due to the vortex motion. However, from  $AC$  susceptibility possible to define the vortex solid to liquid phase transition only at sufficiently low frequency (and low  $AC$  amplitude). This restriction is caused by a significant dependency of the peak position ( $T_p$ ) on  $\chi''$  data from the  $AC$  field frequency and amplitude. When the  $AC$  field frequency is lowered,  $T_p$  shifts towards lower temperatures due to the current density loss compensation during the relaxation [22]. In case the DC field increases, the transition in  $\chi'(T)$  and  $\chi''(T)$  moves to lower temperatures, and the peak height increases to a certain value and then remains more or less constant for further increasing DC magnetic fields. Thus, the  $T_p(H)$

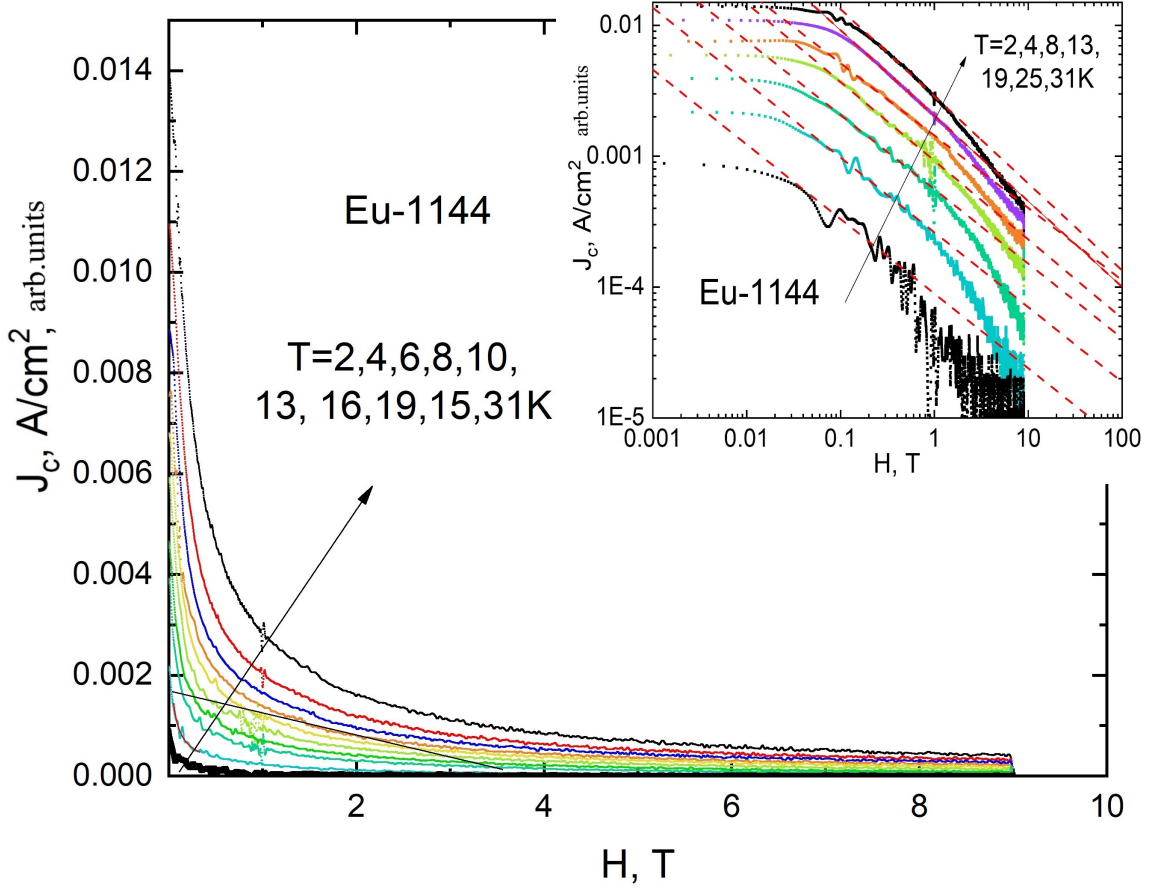


**Figure 4.** Critical current density versus magnetic field with  $H \parallel c$  for Eu-1144. Inset: Eu-1144 log-log plot of the critical current versus magnetic field. The drawn lines show the power law  $B^n$ , whereas  $0.55 < n < 0.65$  expected from the strong pinning contribution.

dependence can be used to determine phase transition line. In Fig.5(a) presented  $\chi''(T)$  AC susceptibility data for various frequencies near the superconducting peak region. Using the criteria of  $T_p$  determination as it was shown in ref. [21] we plot  $T_p(H)$  in Fig.5(b). The  $T_p(H)$  data can be well fitted using the formula:  $H(T_p) = H_0(1 - t_p)^\beta$ ; (2) whereas  $t_p = T_p/T_c$  and exponent  $\beta$  can give us information about the vortex pinning strength [24]. In cuprate superconductors values found in the fitting of the irreversibility line are commonly in the range  $\beta = 4/3 \div 3/2$ . We found that  $\beta$  in Eu-1144 varied from 1.74 at  $f=33$  Hz to 1.91 at  $f=9777$  Hz. A rather high value of  $\beta$  may indicates strong pinning. Similar behaviour was also reported for  $K_{0.8}Fe_2Se_2$  [22],  $FeS_{1-x}Se_x$  [25]. In melt-textured single domain cuprate superconductor (Gd-Ba-Cu-O) variety of  $\beta$  values interpreted in the framework of flux diffusion model [22]. However, the true nature of this phenomenon in iron-based superconductors is still under discussion.

From the AC susceptibility, as it was mentioned above, we found irreversibility line or border of vortex glass to vortex liquid phase transition. The irreversibility was obtained from interpolation of  $1/T_p$  vs  $\nu$  data to low frequency (1Hz) as it is shown on

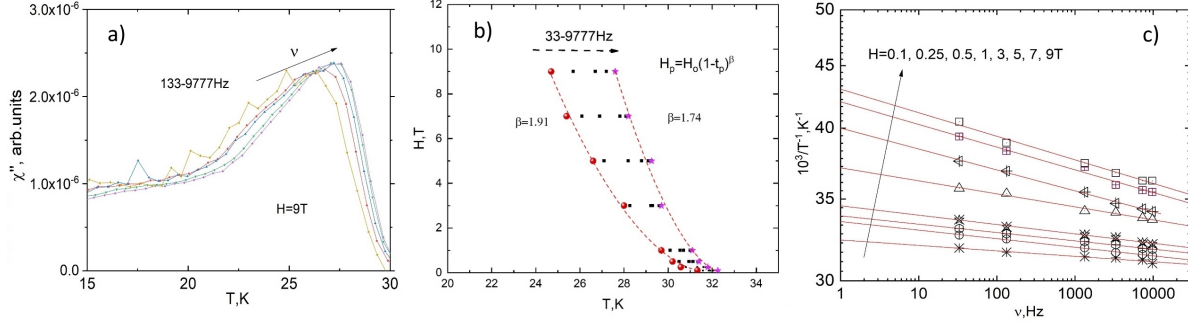


**Figure 5.** a) Temperature dependence of the out-of-phase AC susceptibility with  $H//c$  at  $H=9$  T at various frequencies. b) The  $T_p$  obtained at various frequencies and magnetic fields. The dashed lines are fitting by  $H(T_p) = H_0(1 - t_p)^\beta$  for 133 Hz and 9777 Hz data, respectively. c) Logarithmic  $\nu_m$  dependence of  $1/T_p$  in  $EuRbFe_4As_4$  ( $H_{ac} = 1$  Oe) in various magnetic fields. The red line is the best-fit function according to the Eq.2

Fig.5(c) [21]. Moreover, according to the theory AC-response of susceptibility in the vortex liquid region mainly rises from the thermally activated vortex jumps between metastable states of the vortex lattice [26]. In the vortex solid state, the flux lines have additionally to overcome the pinning potential wells, and a thermally activated flux creep is observed. The main parameter that governs the vortex motion is the effective pinning barrier  $U$ , which is described within a thermally activated framework by the expression [21, 27]:

$$\frac{1}{T_p(\nu)} = -\frac{1}{U_0(H)} \ln\left(\frac{\nu}{\nu_0}\right)$$

(2).

This approximation implies that  $1/T_p$  depends mainly on the  $U_0$  parameter, playing the role of an effective depinning energy barrier in a thermally activated flux creep model. The parameter  $\nu_0$  is the characteristic frequency associated with the motion of vortices (vortex hopping) around their equilibrium position ( $10^{10} - 10^{12}$  Hz) [26].

Calculation of  $U_0(H)$  field dependence from the experimental data is shown in Fig. 6. The effective value of the pinning barrier reaches 6700K at low fields, which is similar to reported values of other iron-based superconductors:  $SmFeAsO_{0.8}F_{0.2}$  ( $\sim 5 \times 10^4 K$ ) [20],  $Ba_{0.72}K_{0.28}Fe_2As_2$  ( $\sim 10^4 K$ ) [28],  $BaFe_{1.9}Ni_{0.1}As_2$  ( $\sim 10^4 K$ ) [23],  $FeS$  ( $\sim 5 \times 10^3 K$ ) [25] and  $FeTe_{0.5}Se_{0.5}$  ( $\sim 10^4 K$ ) [29]. High values of activation energy evident in strong pinning in the  $EuRbFe_4As_4$  superconductor. Furthermore, the field dependence of  $U_0(H)$  displays at least two regimes with a crossover at field about 1T. The theory predicts that a plateau at low fields is associated with single-vortex pinning regime. In higher magnetic fields power law dependence  $U_0 \propto H^{-a}$  may be observed. In this study  $U_0(H)$  follows  $H^{-0.52}$  dependence in the whole measured field. Therefore collective pinning with  $U_0 \sim H^{-1}$  is not the case. The possible mechanism here, considering  $U_0 \sim H^{-0.5}$ , might be thermally activated plastic motion [30] or/and

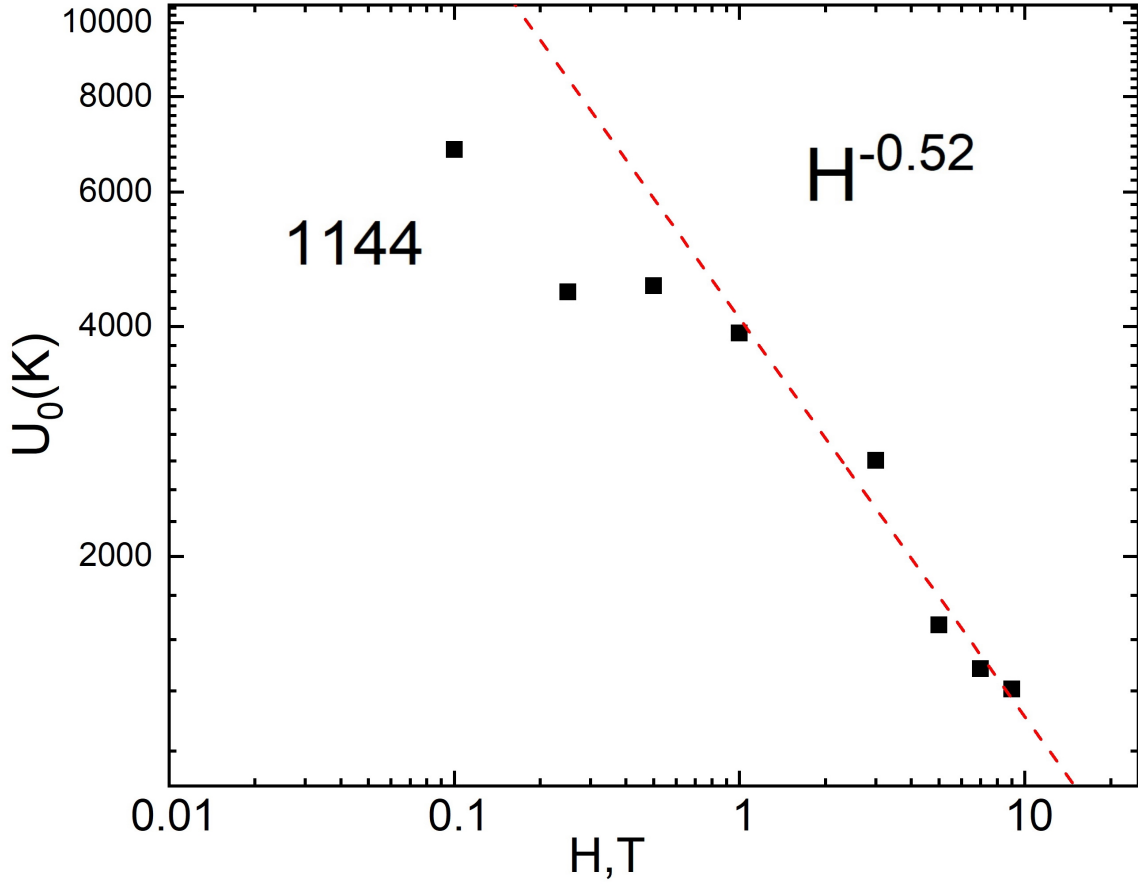


**Figure 6.** Field dependence of the activation energy,  $U_0(H)$  for  $\text{EuRbFe}_4\text{As}_4$ .

flux pinning due to the planar defects [31].

Summarizing data, the magnetic phase diagram of  $\text{EuRbFe}_4\text{As}_4$  was built as shown in Fig. 7. A rough estimation of the  $H_{c2}(T)$  slope near  $T_c$  gives  $dH_{c2}/dT$  values about  $-3.34\text{T/K}^{-1}$  for  $H \parallel ab$  and for  $H \parallel c$  about  $-2.19\text{T/K}^{-1}$ , respectively. Applying Werthamer-Helfand-Hohenberg (WHH) formula, whereas  $H_{c2}(0) = 0.693dH/dT|_{T_c} \times T_c$ , for a type-II superconductor, we found  $H_{c2}^c(0)$  and  $H_{c2}^{ab}(0)$  values 54T and 81T, respectively. Another opportunity to evaluate the upper critical field is to take into account well known spin-paramagnetic pair-breaking effect, which originates from the Zeeman splitting of spin singlet Cooper pairs. The Pauli-limiting field  $H_p$  has derived from the condition that the Zeeman energy in the normal state compensates the superconducting condensation energy under magnetic field [33]. For a conventional BCS (Bardeen-Cooper-Schrieffer) superconductor, where  $2\Delta(0) = 3.52k_B T_c$ ,  $H_p^{BCS}(0) = 1.84T_c$ . Therefore, we found the pair-braking limitation of  $H_{c2}$  about 65T for both field orientations. Considering the WHH,  $H_{c2}$  estimations exceed the BCS paramagnetic limit, the deviations from the GL model may occur [2]. Nevertheless, coherent lengths  $\xi^{ab}$  and  $\xi^c$  were estimated from the single band Ginzburg-Landau equations  $H_{c2}^{ab}(0) = \Phi_0/2\pi\xi_{ab}^2$  and  $H_{c2}^c(0) = \Phi_0/(2\pi\xi_{ab}\xi_c)$ . The estimations yielding  $\xi_{ab} = 2.47\text{nm}$

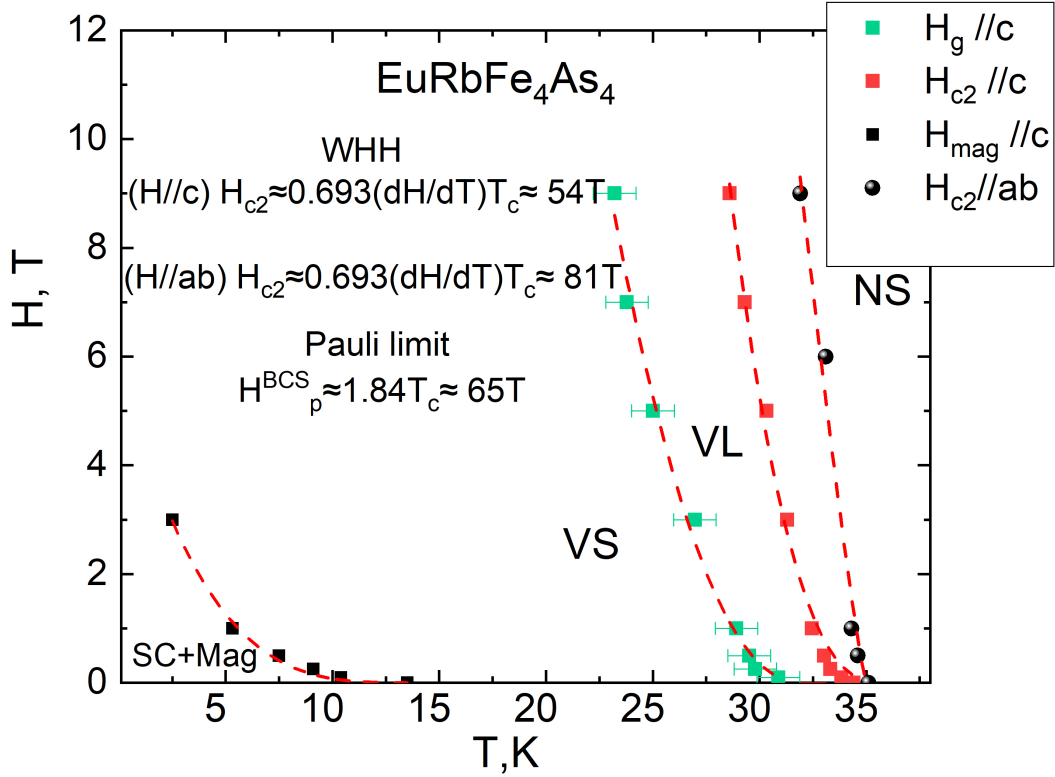


**Figure 7.** Vortex phase diagram of  $\text{EuRbFe}_4\text{As}_4$  single crystal.

and  $\xi_c = 1.65\text{nm}$  respectively. Additionally, we calculate the anisotropy  $\Gamma = H_{c2}^{ab}/H_{c2}^c$  from the  $H_{c2}^{ab}(T)$  and  $H_{c2}^c(T)$  data using linear interpolation. Anisotropy value about 3–4 in a region close to  $T_c$  with a tendency to decrease less than 2 at low temperatures according to WHH estimations. The  $H_{c2}(0)$  values estimated in this work are comparable with the results obtained in ref. [3], but significantly less than in ref. [2]. Their estimated values of upper critical field were about 160T and 250T for  $H_{c2}^c(0)$  and  $H_{c2}^{ab}(0)$ , with  $dH_{c2}^{ab}/dT = -4.2\text{T/K}^{-1}$  and  $dH_{c2}^c/dT = -7\text{T/K}^{-1}$ , respectively. Meanwhile, direct high-field measurements in similar  $\text{CaNaFe}_4\text{As}_4$  superconductor, with  $T_c = 35\text{K}$   $dH_{c2}^{ab}/dT$  about  $-5\text{T/K}^{-1}$  and  $dH_{c2}^c/dT$  about  $-10\text{T/K}^{-1}$  at low field data shows that upper critical field in both cases less than 100T [6]. Therefore, the real values of upper critical field in Eu-1144 should be about or less than 100T, which were very recently demonstrated in direct high field measurements [34]. Authors showed the values of the upper critical field were in the range of 70-80T, which is consistent with our  $H_{c2}(0)$  estimations. It was also concluded that the Pauli limit prevails for  $H \parallel ab$ , but for  $H \parallel c$  orbital limitation was more essential. Moreover, it was assumed that 1144 a possible candidate for existence of the FFLO state. [34].

## 4. Conclusions

In summary, detailed AC susceptibility and magnetic moment measurements were performed to study the vortex pinning and flux dynamics in the  $\text{EuRbFe}_4\text{As}_4$  single crystals. The irreversibility line has been found for Eu-1144, showing rather narrow vortex liquid region. The activation energy come up to 6700K at low fields and indicating strong pinning. The following  $U_0$  decays in the magnetic field as  $H^{-0.52}$  higher than 1T is typical for thermally activated plastic motion. However, considering the layered structure of this material with Eu magnetic layers the flux pinning due to planar defects are also possible. The strong pinning in Eu-1144 was also confirmed by M(H) data. We show that Eu magnetic ordering is fully suppressed at fields about 3T. Summarizing experimental data, we built the magnetic phase diagram of the  $\text{EuRbFe}_4\text{As}_4$  superconductor.

## 5. Acknowledgments

The measurements were done using research equipment of the Shared Facilities Center at LPI.

- [1] A. Iyo, K. Kawashima, T. Kinjo, T. Nishio, S. Ishida, H. Fujihisa, Y. Gotoh, K. Kihou, H. Eisaki, and Y. Yoshida, *J. Am. Chem. Soc.* **138**, 3410 (2016).
- [2] M. P. Smylie, K. Willa, J.-K. Bao, K. Ryan, Z. Islam, H. Claus, Y. Simsek, Z. Diao, A. Rydh, A. E. Koshelev, W.-K. Kwok, D. Y. Chung, M. G. Kanatzidis, and U. Welp, *Phys. Rev. B* **98**, 104503 (2018).
- [3] K. Kawashima, T. Kinjo, T. Nishio, S. Ishida, H. Fujihisa, Y. Gotoh, K. Kihou, H. Eisaki, Y. Yoshida, and A. Iyo, *J. Phys. Soc. Jpn.* **85**, 064710 (2016).
- [4] Y. Liu, Y.-B. Liu, Z.-T. Tang, H. Jiang, Z.-C. Wang, A. Ablimit, W.-H. Jiao, Q. Tao, C.-M. Feng, Z.-A. Xu, and G.-H. Cao, *Phys. Rev. B* **93**, 214503 (2016).
- [5] Kenji Kawashima, Shigeyuki Ishida, Hiroshi Fujihisa, Yoshito Gotoh, Kunihiro Kihou, Yoshiyuki Yoshida, Hiroshi Eisaki, Hiraku Ogino, and Akira Iyo, *J. Phys. Chem. Lett.*, **9**, 868873 (2018).
- [6] W. R. Meier, T. Kong, U. S. Kaluarachchi, V. Taufour, N. H. Jo, G. Drachuck, A. E. Bhmer, S. M. Saunders, A. Sapkota, A. Kreyssig, M. A. Tanatar, R. Prozorov, A. I. Goldman, Fedor F. Balakirev, Alex Gurevich, S. L. Bud'ko, and P. C. Canfield, *Phys. Rev. B* **94**, 064501 (2016).
- [7] Shiv J. Singh, Matthew Bristow, William R. Meier, Patrick Taylor, Stephen J. Blundell, Paul C. Canfield, and Amalia I. Coldea, *Phys. Rev. Mat.* **2**, 074802 (2018).
- [8] K. Kawashima, S. Ishida, K. Oka, H. Kito, N. Takeshita, H. Fujihisa, Y. Gotoh, K. Kihou, H. Eisaki, Y. Yoshida, and A. Iyo, *J. Phys.: Conf. Ser.* **969**, 012027 (2018).
- [9] K S Pervakov, V A Vlasenko, E P Khlybov, A Zaleski, V M Pudalov and Yu F Eltsev, *Supercond. Sci. Technol.* **26** 015008 (2013).
- [10] T E Kuzmicheva, A V Muratov, S A Kuzmichev, A V Sadakov, Yu A Aleshchenko, V A Vlasenko, V P Martovitsky, K S Pervakov, Yu F Eltsev, V M Pudalov, *Phys. Usp.* **60** 419429 (2017).
- [11] Jin-Ke Bao, Kristin Willa, Matthew P. Smylie, Haijie Chen, Ulrich Welp, Duck Young Chung, and Mercouri G. Kanatzidis, *Cryst. Growth Des.* **18**, 6, 3517-3523 (2018).
- [12] Yi Liu, Ya-Bin Liu, Ya-Long Yu, Qian Tao, Chun-Mu Feng, and Guang-Han Cao, *Phys. Rev. B* **96**, 224510 (2017).
- [13] Mohammed A. Albedah, Farshad Nejadstattari, Zbigniew M. Stadnik, Yi Liu, and Guang-Han Cao, *Phys. Rev. B* **97**, 144426 (2018).

- [14] V. S. Stolyarov, A. Casano, M. A. Belyanchikov, A. S. Astrakhantseva, S. Y. Grebenchuk, D. S. Baranov, I. A. Golovchanskiy, I. Voloshenko, E. S. Zhukova, B. P. Gorshunov, A. V. Muratov, V. V. Dremov, L. Y. Vinnikov, D. Roditchev, Y. Liu, G. H. Cao, M. Dressel, and E. Uykur, *Phys. Rev. B* **98**, 140506(R) (2018).
- [15] C.P. Bean, *Rev. Mod. Phys.* **36**, 31 (1964).
- [16] V. K. Vlasko-Vlasov, A. E. Koshelev, M. Smylie, J.-K. Bao, D. Y. Chung, M. G. Kanatzidis, U. Welp, and W.-K. Kwok *Phys. Rev. B* **99**, 134503 Published 3 April 2019 (Supplementary material).
- [17] N. Haberkorn, M. Miura, B. Maiorov, G. F. Chen, W. Yu, and L. Civale, *Phys. Rev. B* **84**, 094522 (2011).
- [18] N. Haberkorn, B. Maiorov, I. O. Usov, M. Weigand, W. Hirata, S. Miyasaka, S. Tajima, N. Chikumoto, K. Tanabe, and Leonardo Civale, *Phys. Rev. B* **85**, 014522 (2012).
- [19] C. J. van der Beek, G. Rizza, M. Konczykowski, P. Fertey, I. Monnet, Thierry Klein, R. Okazaki, M. Ishikado, H. Kito, A. Iyo, H. Eisaki, S. Shamoto, M. E. Tillman, S. L. Budko, P. C. Canfield, T. Shibauchi, and Y. Matsuda, *Phys. Rev. B* **81**, 174517 (2010).
- [20] G. Prando, P. Carretta, R. De Renzi, S. Sanna, A. Palenzona, M. Putti, and M. Tropeano, *Phys. Rev. B* **83**, 174514 (2011).
- [21] G. Prando, P. Carretta, R. De Renzi, S. Sanna, H. J. Grafe, S. Wurmehl, and B. Buchner, *Phys. Rev. B* **85**, 144522 (2012).
- [22] Junyi Ge, Joffre Gutierrez, Mingtao Li, Jincang Zhang, and Victor V. Moshchalkov, *Appl. Phys. Lett.* **103**, 052602 (2013).
- [23] Jun-Yi Ge, Lin-Jun Li, Zhu-An Xu, and Victor V. Moshchalkov, *Journal of Applied Physics* **119**, 163904 (2016).
- [24] Y. Yeshurun and A. P. Malozemoff, *Phys. Rev. Lett.* **60**, 2202 (1988).
- [25] Aifeng Wang and C. Petrovic, *Appl. Phys. Lett.* **110**, 232601 (2017).
- [26] G. Blatter, M.V. Feigelman, V.B. Geshkenbein, A.I. Larkin, V.M. Vinokur, *Rev. Mod. Phys.* **66**, 1125 (1994).
- [27] M. Buchacek, R. Willa, V. B. Geshkenbein, and G. Blatter, *Phys. Rev. B* **98**, 094510 (2018).
- [28] E. Bellingeri, S. Kawale, I. Pallecchi, A. Gerbi, R. Buzio, V. Braccini, A. Palenzona, M. Putti, M. Adamo, E. Sarnelli, and C. Ferdeghini, *Appl. Phys. Lett.* **100**, 082601 (2012).
- [29] X.-L. Wang, S. R. Ghorbani, S.-I. Lee, S. X. Dou, C. T. Lin, T. H. Johansen, K.-H. Muller, Z. X. Cheng, G. Peleckis, M. Shabazi, A. J. Qviller, V. V. Yurchenko, G. L. Sun, and D. L. Sun, *Phys. Rev. B* **82**, 024525 (2010).
- [30] V. M. Vinokur, M. V. Feigelman, V. B. Geshkenbein, and A. I. Larkin, *Phys. Rev. Lett.* **65**, 259 (1990).
- [31] E. Bartolom, A. Palau, A. Llord, T. Puig, and X. Obradors, *Phys. Rev. B* **81**, 184530 (2010).
- [32] N. R. Werthamer, E. Helfand, and P. C. Hohenberg *Phys. Rev.* **147**, 295 (1966).
- [33] S. Khim, B. Lee, J. W. Kim, E. S. Choi, G. R. Stewart, and K. H. Kim *Phys. Rev. B* **84**, 104502 (2011).
- [34] M. P. Smylie, A. E. Koshelev, K. Willa, R. Willa, W.-K. Kwok, J.-K. Bao, D. Y. Chung, M. G. Kanatzidis, J. Singleton, F. F. Balakirev, H. Hebbeker, P. Niraula, E. Bokari, A. Kayani, and U. Welp, *arXiv:1904.07203v2* [cond-mat.supr-con] 16 Apr (2019).